IMMUNOLOGY

Blocking FcRn in humans reduces circulating IgG levels and inhibits IgG immune complex–mediated immune responses

L. J. Blumberg[1], J. E. Humphries[2], S. D. Jones[3], L. B. Pearce[2], R. Holgate[4], A. Hearn[4], J. Cheung[5], A. Mahmood[5], B. Del Tito[2], J. S. Graydon[1]*, L. E. Stolz[1†], A. Bitonti[1], S. Purohit[3], D. de Graaf[1‡], K. Kacena[6], J. T. Andersen[7,8], G. J. Christianson[9], D. C. Roopenian[9], J. J. Hubbard[10,11], A. K. Gandhi[10], K. Lasseter[12], M. Pyzik[10], R. S. Blumberg[10§]

The neonatal crystallizable fragment receptor (FcRn) functions as an intracellular protection receptor for immunoglobulin G (IgG). Recently, several clinical studies have reported the lowering of circulating monomeric IgG levels through FcRn blockade for the potential treatment of autoimmune diseases. Many autoimmune diseases, however, are derived from the effects of IgG immune complexes (ICs). We generated, characterized, and assessed the effects of SYNT001, a FcRn-blocking monoclonal antibody, in mice, nonhuman primates (NHPs), and humans. SYNT001 decreased all IgG subtypes and IgG ICs in the circulation of humans, as we show in a first-in-human phase 1, single ascending dose study. In addition, IgG IC induction of inflammatory pathways was dependent on FcRn and inhibited by SYNT001. These studies expand the role of FcRn in humans by showing that it controls not only IgG protection from catabolism but also inflammatory pathways associated with IgG ICs involved in a variety of autoimmune diseases.

INTRODUCTION

The recognition that immunoglobulin G (IgG) autoantibodies can have pathogenic effects has stimulated the development of numerous strategies aimed at removing or decreasing the effects of IgG and its associated immune complexes (ICs) (1, 2). Preclinical data support the notion that blockade of the neonatal Fc receptor (FcRn) may also serve as a unique treatment for IgG-mediated autoimmune diseases (3–7). FcRn is a major histocompatibility complex (MHC) class I–related molecule that associates noncovalently with β_2-microglobulin (β_2m) (8). Despite its name, it is now well recognized that FcRn is widely expressed throughout human life in multiple types of parenchymal (9–11) and hematopoietic cells (12–15). FcRn functions within intracellular endosomes, where it binds IgG and albumin at distinct, nonoverlapping sites under acidic but not neutral pH conditions (16). Thus, FcRn is considered a saturable "protection" receptor that serves to prevent the catabolism of IgG and albumin (8). It does so through its ability to bind these two proteins within early and recycling acidic endosomes whereby it diverts them from destruction in lyso-

somes, lastly returning these cargo molecules to the neutral pH of the cell surface where they are released (17–19). This process accounts for the unusually long half-life of circulating IgG and albumin (8) and is likely the basis for many of the therapeutic benefits of intravenous immunoglobulin (IVIG) as exogenously administered antibodies have been suggested to compete for FcRn binding resulting in its saturation and lowering of endogenous IgG levels (6).

Mouse studies illustrate that FcRn expression in cells of bone marrow origin contributes to the protection of not only circulating monomeric IgG (13, 20, 21) but also circulating ICs (CICs) such that when FcRn is absent from hematopoietic cells, CICs are eliminated more rapidly from the bloodstream (22). In addition to regulating CIC levels, FcRn in Ag-presenting cells (APCs) also determines the ability of IgG ICs to promote the secretion of inflammatory cytokines (23) and their intracellular routing to compartments critical to Ag processing and presentation via MHC class II to CD4$^+$ T cells and cross-presentation via MHC class I to CD8$^+$ T cells (22, 24). Consistent with this, genetic deletion or pharmacologic inhibition of FcRn protects from autoimmune diseases in mouse models (4, 6, 7). This suggests that FcRn functions broadly in inflammatory pathways by preventing the degradation of IgG and IgG ICs and enabling IgG ICs to mediate innate and adaptive immune functions.

Although several approaches to directly blocking FcRn for the potential treatment of autoimmunity have recently emerged (25–27), they have exclusively focused on the reduction of circulating monomeric IgG levels and have not considered the possible impact that FcRn has on immune response to IgG ICs. Here, we report a humanized, affinity-matured IgG4-κ monoclonal antibody, SYNT001, that specifically interferes with human FcRn (hFcRn) binding to IgG and describe its pharmacokinetic (PK), pharmacodynamic (PD), and safety profile in cynomolgus monkeys and healthy human volunteers. In doing so, we reveal that blockade of FcRn rapidly lowers the levels of CICs in humans and the ability of IgG ICs to induce inflammatory responses by hematopoietic cells.

[1]Syntimmune Inc., Boston, MA 02116, USA. [2]Biologics Consulting, Alexandria, VA 22314, USA. [3]BioProcess Technology Consultants, Woburn, MA 01801, USA. [4]Abzena, Babraham, Cambridge, CB22 3AT, UK. [5]New York Structural Biology Center, New York, NY 10027, USA. [6]BioBridges, Wellesley, MA 02481, USA. [7]Department of Immunology and Centre for Immune Regulation, Oslo University Hospital Rikshospitalet and University of Oslo, Oslo 0424, Norway. [8]Department of Pharmacology, Institute of Clinical Medicine, University of Oslo, Oslo 0424, Norway. [9]The Jackson Laboratory, Bar Harbor, ME 04609, USA. [10]Department of Medicine, Division of Gastroenterology, Hepatology and Endoscopy, Brigham and Women's Hospital, Harvard Medical School, Boston, MA 02115, USA. [11]Department of Medicine, Division of Gastroenterology, Hepatology and Nutrition, Boston Children's Hospital, Boston, MA 02115, USA. [12]Clinical Pharmacology of Miami, Miami, FL 33014, USA.
*Present address: Alexion Pharmaceuticals Inc., 121 Seaport Blvd., Boston, MA 02210, USA.
†Present address: Verve Therapeutics Inc., 26 Landsdowne St., Cambridge, MA 02139, USA.
‡Present address: Comet Therapeutics, 610 Main Street, Cambridge, MA 02139, USA.
§Corresponding author. Email: rblumberg@bwh.harvard.edu

RESULTS

Development and characterization of SYNT001 in mice

We developed a humanized, affinity-matured, deimmunized IgG4-κ monoclonal antibody (SYNT001) containing a S241P mutation that binds hFcRn at neutral and acidic pH (Table 1). The cocrystal structure of hFcRn in complex with a SYNT001-derived Fab fragment was solved to a resolution of 2.4 Å (table S1) and showed binding in a 1:1 stoichiometric ratio by engaging residues 85 to 88, 112 to 117, and 130 to 133 on the hFcRn α heavy chain and residues 1 to 3 and 58 to 60 on the β2m light chain (Fig. 1A and fig. S1A). This binding surface completely overlaps with that of IgG1 Fc binding to the hFcRn α chain and β2m (Fig. 1, B and C) and is distinct from the albumin binding site (fig. S1A).

Immunohistochemistry showed that SYNT001 bound to the expected hematopoietic, endothelial, and epithelial cells in a wide variety of tissues consistent with previous observations (fig. S1B) (8, 28, 29) and identified several cells and tissues previously unrecognized to express FcRn. The latter included the epithelium of the bladder, parathyroid gland, pituitary gland, and platelets (Fig. 1D).

SYNT001 promoted clearance of human IgG (hIgG) antibodies and IgG ICs in vivo as shown in mice expressing hFcRn ($FCGRT^{TG/-}Fcgrt^{-/-}$). As $FCGRT^{TG/-}Fcgrt^{-/-}$ mice, due to the low affinity of hFcRn for mouse IgG, are hypogammaglobulinemic (30), IVIG was administered together with a chimeric humanized antibody (HuLys11) to directly trace hIgG in a physiologic milieu (fig. S1C) (31). Treatment with SYNT001 (20 mg/kg) significantly reduced the plasma concentration of HuLys11 compared with the vehicle-treated control group [area under curve of vehicle ($AUC_{Vehicle}$), 256.6 ± 17.72; $AUC_{SYNT001}$, 116 ± 21.01%, which represent of HuLys11 remaining*time] (Fig. 1E). ICs were examined using hapten, 4-hydroxy-3-iodo-5-nitrophenylacetic acid (NIP), conjugated ovalbumin (OVA^{NIP}) as a model Ag and an anti-NIP hIgG1 antibody ($hIgG1^{WT}$) (24). $hIgG1^{WT}$ ICs were administered to $FCGRT^{TG/-}Fcgrt^{-/-}$ mice as previously described (fig. S1D) (22). SYNT001 (20 mg/kg) significantly accelerated CIC removal ($AUC_{Vehicle}$, 345.5 ± 43.05; $AUC_{SYNT001}$, 117 ± 5.424% of $hIgG1^{WT}$ IC remaining*time) compared with mice receiving vehicle, in which the CIC persisted (Fig. 1F).

We also treated primary CD11c$^+$ APCs from $B2M^{TG/TG}FCGRT^{TG/TG}Fcgrt^{-/-}$ mice expressing hFcRn/hβ2m with OVA^{NIP} containing ICs derived from either anti-NIP $hIgG1^{WT}$ antibodies or anti-NIP hIgG1 antibodies that maintain Fcγ receptor (FcγR) binding but are unable to engage FcRn ($hIgG1^{IHH}$) (22, 24) in the presence of increasing concentrations of SYNT001 or isotype control. SYNT001, but not isotype

control, inhibited the ability of the APCs to stimulate interferon-γ (IFN-γ) secretion by OVA-specific CD8$^+$ (Fig. 1G) and CD4$^+$ T cells (Fig. 1H). We observed comparable results with F(ab′)2 fragments of SYNT001 and IgG4 isotype control antibodies (fig. S1, E and F), together indicating that SYNT001 can impede IgG IC activation of the FcRn-mediated adaptive immune function.

SYNT001 reduces IgG in cynomolgus monkeys

We used NHPs as a pharmacologically relevant model for conducting Good Laboratory Practice toxicology studies as SYNT001 demonstrated similar binding to primate and hFcRn (Table 1). Male ($n = 4$ or 6) and female ($n = 4$ or 6) cynomolgus monkeys received five weekly bolus intravenous doses of 10, 30, or 100 mg/kg of SYNT001, which caused dose-dependent and specific reduction of total circulating levels of IgG (Fig. 2A) but not albumin (Fig. 2B), IgA (Fig. 2C), or IgM (Fig. 2D). SYNT001 administration resulted in a maximal 71 ± 7% reduction in IgG levels within 3 to 4 days after the second dose (100 mg/kg), an effect that was completely reversible by its return to baseline at a rate of 2.6% per day following treatment discontinuation (Fig. 2A).

We performed PK analysis after the first (day 1) and fifth (day 29) doses of SYNT001 as summarized in Table 2. C_{max} (maximum observed concentration), $AUC_{(0–144h)}$ (AUC from time 0 to 144 hours), and $T_{1/2}$ (half-life) increased in a dose proportional manner between 10 and 100 mg/kg. The apparent volume of distribution at steady state (V_{ss}) approximated the plasma volume after the first dose (28.6 to 29.8 ml/kg). Repeated administration was associated with reductions in C_{max} and $AUC_{(0–144h)}$ that were inversely dependent on dose as evidenced by a 71% decrease in exposure at 10 mg/kg but only a 32% decrease at 100 mg/kg (Table 2 and Fig. 2E). This was consistent with the presence of anti-SYNT001 antidrug antibodies (ADAs) in NHP serum that developed by day 15 in all monkeys with an apparent reduction in the PD effect after administration of the third dose in the 10 and 30 mg/kg dose groups (Fig. 2E). This trend, however, was not observed in 100 mg/kg dose cohort, which maintained a maximal PD effect through the duration of the study (Fig. 2A), in accordance with the ability to dose through the ADA (32).

Immunophenotyping by flow cytometry revealed no change in the relative percentages and absolute quantities of white blood cells including total T cells, CD4$^+$ and CD8$^+$ T cells, B cells, natural killer cells, or monocytes (fig. S2A) as well as platelets (fig. S2B). In addition, we followed FcRn expression during SYNT001 treatment of NHPs through cell surface and intracellular staining by focusing on monocytes that have been reported to distinctively express high FcRn levels on the cell surface in humans (12). To do so, we used a mouse anti-hFcRn monoclonal antibody, ADM31, which cross-reacts with NHP FcRn (33) and blocks FcRn-albumin (11), but not FcRn-IgG (34) interactions, making it distinct from SYNT001 binding interface. ADM31 could detect the presence of FcRn on the surface of human blood monocytes, dendritic cells (DCs), and neutrophils, while lymphocytes were mostly negative (Fig. 2, F and G). In NHPs, we found that although FcRn staining of the monocyte surface decreased following SYNT001 administration and returned to baseline before subsequent doses (Fig. 2H, top), no significant changes in total FcRn staining were observed (Fig. 2H, bottom), suggesting that SYNT001 administration caused FcRn internalization but not enhanced degradation. Last, the SYNT001 PD effects were not associated with organ toxicity of study animals at all doses such that the no observed adverse effect level was the highest dose tested (100 mg/kg).

Table 1. Binding kinetics of SYNT001 to human and primate FcRn at different pH values. pFcRn, cynomolgus monkey FcRn.

Type of FcRn	K_a (10^4/Ms)	K_d (10^{-4}/s)	K_D (nM)*
	pH 7.4		
hFcRn	35.6 ± 0.3	2.93 ± 0.08	1.19 ± 0.06
pFcRn	4.7 ± 0.1	5.6 ± 0.0	11.9
	pH 6.0		
hFcRn	43.6 ± 1.6	2.71 ± 0.56	0.87 ± 0.2
pFcRn	2.2 ± 0.2	5.1 ± 0.4	23.2

*The kinetic rate constants were obtained using a simple first-order (1:1) Langmuir bimolecular interaction model. The kinetic values represent the average of duplicates.
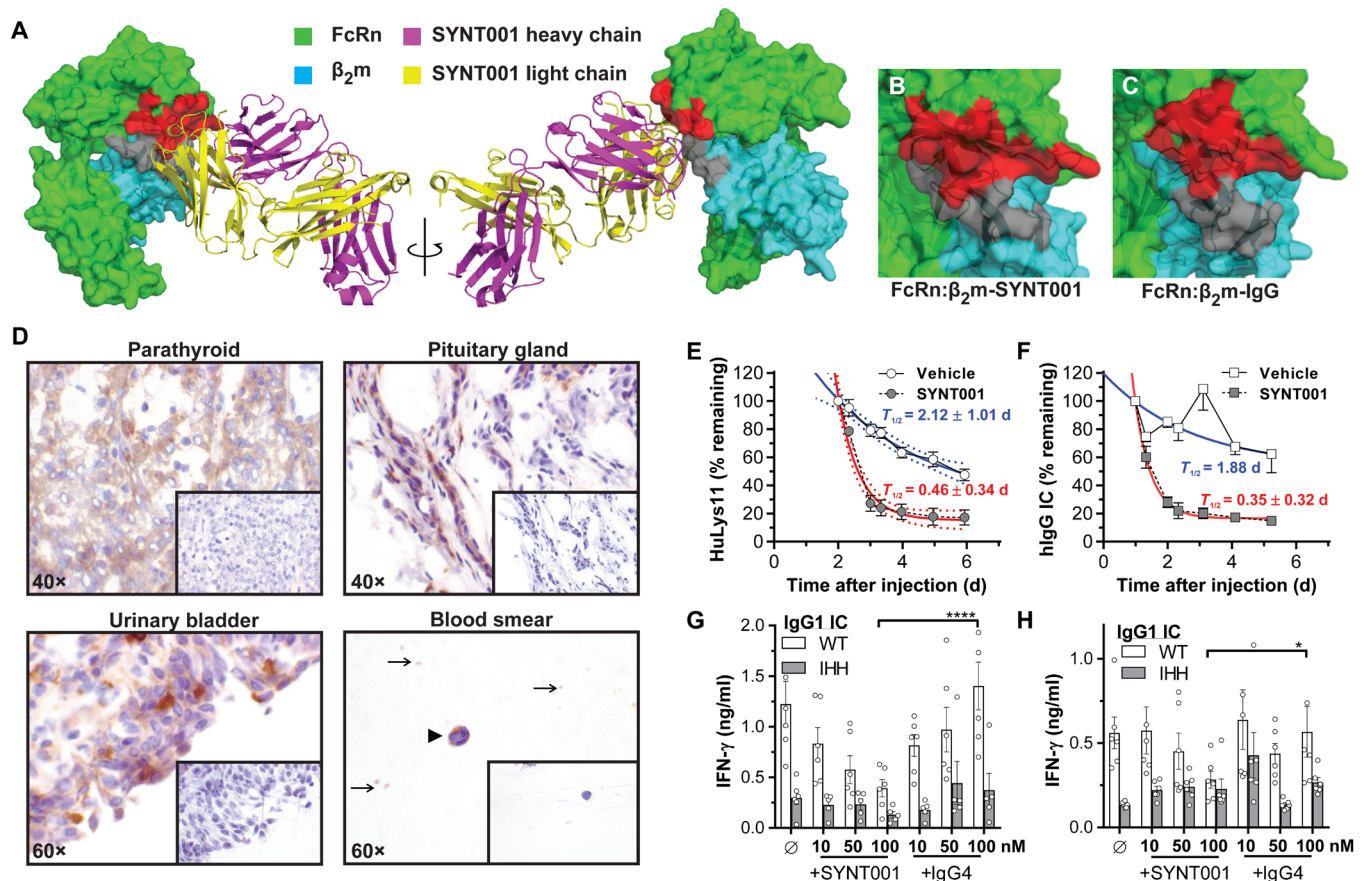
Fig. 1. Characterization of SYNT001. (**A**) Three-dimensional representation of SYNT001 bound to hFcRn. The FcRn α chain and β$_2$m are shown as space-filling model in green and cyan, respectively, while SYNT001 Fab heavy and light chains are shown as ribbon diagrams in magenta and yellow, respectively. SYNT001 contacts both the hFcRn α chain (red) and β$_2$m (gray). (**B**) Magnified image of hFcRn:β$_2$m-SYNT001 interface as shown in (A). SYNT001 makes interactions with the hFcRn α chain (red) and β$_2$m (gray). This interface overlaps with (**C**) the hFcRn:β$_2$m-IgG interface. (**D**) Representative immunohistochemistry images of FcRn staining in the human parathyroid, urinary bladder, pituitary gland, or blood smears (black arrowhead represents monocytes, and black arrows indicate platelets). Insets show negative controls with isotype antibody staining. (**E**) Effect of SYNT001 administration on hIgG levels in $FCGRT^{TG/-}Fcgrt^{-/-}$ mice ($n = 10$) as compared to vehicle treatment. Results are presented as means ± SEM percentage of HuLys11 remaining at indicated time points based on the 48-hour baseline. Curves represent a nonlinear regression analysis with 95% confidence intervals and the half-life ($T_{1/2}$ ± SD) for both groups is indicated. (**F**) Effect of SYNT001 administration on CIC levels in $FCGRT^{TG/-}Fcgrt^{-/-}$ mice as compared to vehicle treatment (vehicle, $n = 10$; SYNT001, $n = 9$). Results are presented as means ± SEM percentage of hIgG ICs remaining at indicated time points based on the 24-hour baseline. Curves represent a nonlinear regression analysis with 95% confidence intervals, and the half-life ($T_{1/2}$ ± SD) for both groups is indicated. (**G**) Effect of SYNT001 on IgG IC cross-presentation. CD11c$^+$ APCs from $B2M^{TG/TG}FCGRT^{TG/TG}Fcgrt^{-/-}$ mice were pretreated with hIgG1^{WT} or hIgG1^{IHH} IC variants in presence of SYNT001 or IgG4 isotype control, followed by coculture with MHC class I–restricted, OVA-specific CD8$^+$ T cells. Forty-eight hours later, IFN-γ production was measured by enzyme-linked immunosorbent assay (ELISA). Means ± SEM is depicted with open circles representing actual data points. (**H**) Effect of SYNT001 on IgG IC presentation. CD11c$^+$ APCs treated as in (G) were cocultured with MHC class II–restricted, OVA-specific CD4$^+$ T cells. Forty-eight hours later IFN-γ production was measured by ELISA. Means ± SEM is depicted with open circles representing actual data points. (G and H) *$P < 0.05$, ****$P < 0.0001$ by two-way analysis of variance (ANOVA) with Fisher's least significant difference (LSD) post hoc test. All experiments with mice were repeated at least twice. WT, wild type.

Clinical study of SYNT001

We conducted a single-center, double-blind, randomized (6:2), single ascending dose, first-in-human study to assess the safety, PK, and PD effects of SYNT001 in healthy human individuals. Thirty-one male individuals (Table 3) were randomized to receive a single intravenous dose of SYNT001 at 1 mg/kg ($n = 6$), 3 mg/kg ($n = 6$), 10 mg/kg ($n = 6$), 30 mg/kg ($n = 5$), or placebo ($n = 8$).

SYNT001 safety profile

No deaths, serious adverse events, or treatment-emergent adverse events (TEAEs) that led to discontinuation of study drug were observed. A total of nine individuals (eight pooled SYNT001 and one placebo) experienced at least one TEAE (Table 4). All TEAEs were

reported in the 10 and 30 mg/kg dose groups. The most common TEAE was headache. One individual in the SYNT001 10 mg/kg dose group experienced a moderate (TEAE grade 2) headache, while the remaining seven individuals experienced mild (TEAE grade 1) headaches. One mild headache was treated with a single dose of acetaminophen; all other headaches resolved without treatment. No other TEAEs were experienced by more than one individual receiving SYNT001. There were no grade 3 or 4 TEAEs and no clinically significant changes in urinalysis, hematology, pulse oximetry, or blood chemistry results. Overall, there was no evidence of dose-limiting adverse reactions up to a maximum dose of SYNT001 (30 mg/kg), together indicating that a single intravenous infusion was well tolerated in healthy volunteers.
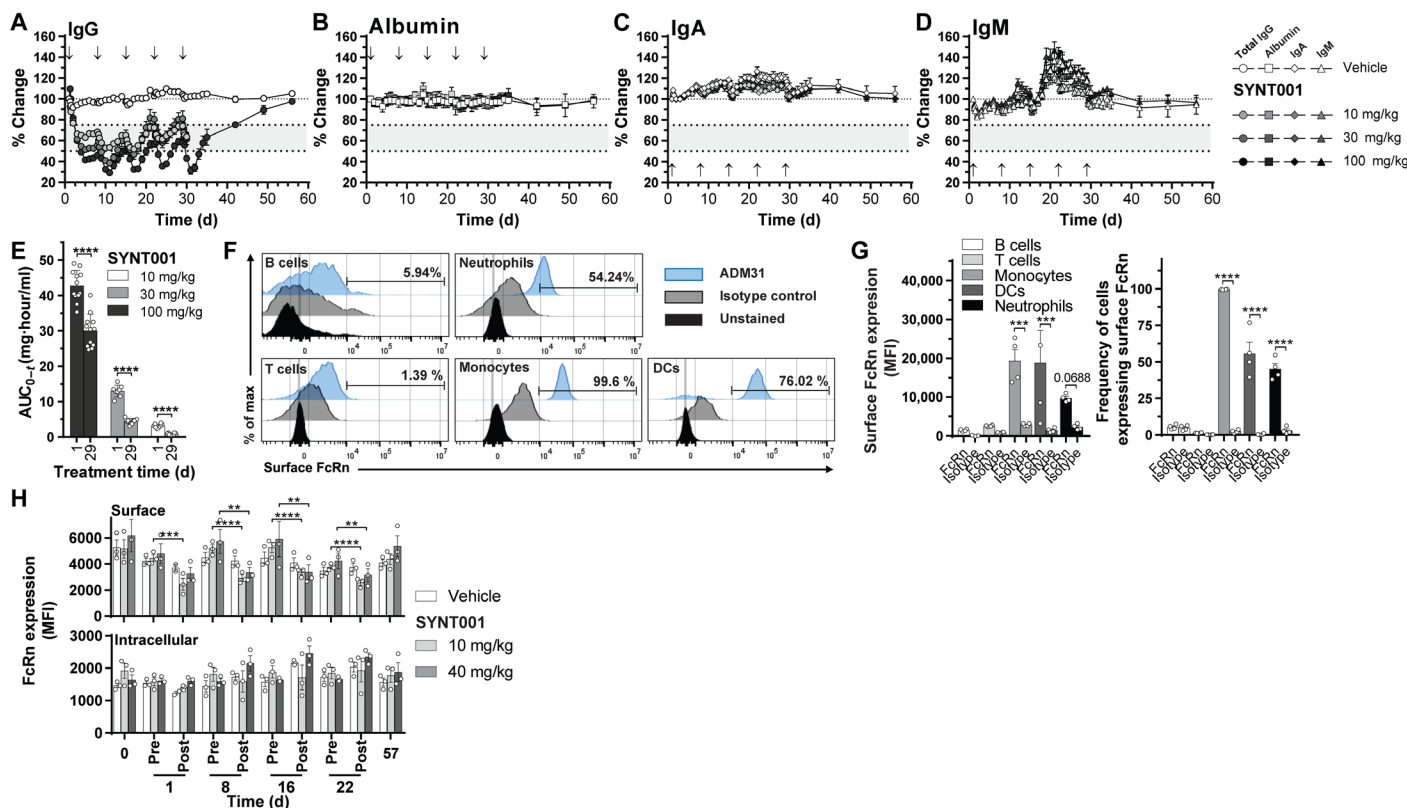
Fig. 2. The effect of repeated-dose SYNT001 administration in cynomolgus monkeys. Mean percentage change in serum concentration of total (**A**) IgG, (**B**) albumin, (**C**) IgA, and (**D**) IgM in cynomolgus monkeys following intravenous administration of repeated-dose SYNT001 at 0 (vehicle), 10, 30, and 100 mg/kg ($n = 8$ in the 10 and 30 mg/kg groups; $n = 12$ in the vehicle and 100 mg/kg groups). Arrows indicate vehicle or SYNT001 administration. Fine dotted lines correspond to baseline levels. Bold dotted lines correspond to 75 and 50% change levels with shaded area in between. (**E**) Summary of effects of repeated dosing on SYNT001 AUC at study days 1 and 29. Symbols represent actual data points from each individual animal. Leukocytes from healthy volunteers were stained for surface FcRn expression with anti-hFcRn antibody (ADM31) or IgG2b isotype control and antibodies for markers identifying the indicated cell subsets. (**F**) Representative histograms from one individual and (**G**) cumulative surface FcRn mean fluorescence intensity (MFI) levels (left) and percentage of cells expressing FcRn (right) are shown. Means ± SEM is depicted with open circles representing each individual. (**H**) Cell surface (top) and intracellular (bottom) FcRn staining of monocytes pretreated and 2-hour posttreated SYNT001 at 0 (vehicle), 10, and 40 mg/kg doses ($n = 3$ per group). Means ± SEM of MFI is depicted. (A) Mixed-effects model repeated-measurement (MMRM) modeling indicated statistical significance ($P < 0.05$) of IgG reduction by SYNT001 in the 10, 30, and 100 mg/kg dose groups compared to vehicle from days 3 to 30. (E) ****$P < 0.0001$ by unpaired Student's t test; (G) ***$P = 0.0007$, ****$P < 0.0001$ by two-way ANOVA with Fisher's LSD post hoc test; (H) **$P < 0.01$, ****$P < 0.0001$ by two-way ANOVA with Fisher's LSD post hoc test.

Pharmacokinetics

A summary of the SYNT001 mean PK parameters is shown in Table 5. The geometric mean values for $AUC_{(0-inf)}$ (AUC extrapolated from time 0 to infinity) increased approximately 8.7- and 41.2-fold for the SYNT001 10 and 30 mg/kg groups, respectively, compared to the 3 mg/kg group. The mean values for C_{max} increased 4-, 16-, and 51-fold for the 3, 10, and 30 mg/kg groups, respectively, compared to the group given 1 mg/kg. When all dose groups were included, a nonlinear power model revealed proportionality coefficients for C_{max} and $AUC_{(0-inf)}$ of 1.16 (90% confidence intervals, 1.10 to 1.23) and 1.65 (90% confidence intervals, 1.55 to 1.76), respectively. This provided confirmation that both C_{max} and AUC increased in a greater than dose proportional manner as expected on the basis of the nonlinear kinetics (Fig. 3A).

The serum concentrations of SYNT001 peaked at 0.08 hours, and the $T_{1/2}$ increased with increasing dose from 0.64 to 7.79 hours over the dose range of 1 to 30 mg/kg (Table 5). As observed for NHPs (Table 2), the mean V_d for SYNT001 approximated the expected plasma compartment volume and ranged from 15.4 to 23.0 ml/kg. Accordingly, clearance (C_L) ranged from 19.0 to 1.9 ml/hour per kg

and was inversely proportional to dose. The increasing $T_{1/2}$ and decreasing C_L with dose were consistent with the fact that semi-log plots showed evidence of nonlinearity in the lower dose groups associated with lower serum concentrations (Fig. 3A). Thus, the data indicate accelerated clearance of SYNT001 at lower serum concentrations, predicting that elimination was occurring because of target-mediated drug disposition via FcRn binding as supported by studies of monocytes in NHPs (Fig. 2H).

Pharmacodynamics

The entry criteria required individuals to have baseline total IgG levels greater than 1200 mg/dl with a study stopping rule when the level fell below the lower limit of normal (LLN; 768 mg/dl) in any individual. SYNT001 caused a dose-dependent decrease in total serum IgG concentrations in individuals who received a single dose of 1, 3, 10, and 30 mg/kg intravenously compared to individuals who received placebo (Fig. 3B and fig. S3A). The median peak effect was observed in the 30 mg/kg dose group with a −46.21% [interquartile range (IQR), −47.40 to −43.36%] change from baseline within 5 days after dosing. On day 28, the total IgG levels had mostly returned to

Table 2. Summary of PK parameter estimates in cynomolgus monkeys treated with SYNT001. T_{max}, time to reach maximum concentration; C_L, clearance; R_{AUC}, ratio of $AUC_{(0-29)}$ to $AUC_{(0-1)}$.

Day	Dose group (mg/kg)	n	C_{max} (μg/ml)	$AUC_{(0-144h)}$ (μg·hour/ml)	$T_{1/2}$ (hours)	V_{SS} (ml/kg)	C_L (ml/hour/kg)	R_{AUC}
	10	8	289 ± 33	3200 ± 559	3.24 ± 0.18	28.6 ± 4.25	3.22 ± 0.579	—
1	30	8	904 ± 95	13200 ± 1770	7.36 ± 1.88	28.8 ± 2.18	2.30 ± 0.327	—
	100	12	3530 ± 614	43700 ± 4650	9.99 ± 1.76	29.8 ± 4.20	2.31 ± 0.250	—
	10	8	186 ± 48	917 ± 318	4.14 ± 1.19	78.3 ± 12.4	11.5 ± 3.99	0.290
29	30	8	716 ± 326	4580 ± 906	3.96 ± 1.71	51.6 ± 14.5	6.80 ± 1.52	0.361
	100	12	3260 ± 402	31200 ± 5180	6.28 ± 2.20	25.9 ± 6.38	3.28 ± 0.486	0.679

Table 3. Summary of demographics—PK population. Note that percentage was calculated with total number of individuals as the denominators for each cohort, respectively.

	Vehicle	SYNT001 (1 mg/kg)	SYNT001 (3 mg/kg)	SYNT001 (10 mg/kg)	SYNT001 (30 mg/kg)	Pooled SYNT001
Enrolled individuals, n (%)	8 (25.8)	6 (19.4)	6 (19.4)	6 (19.4)	5 (16.1)*	23 (74.2)
Completed study	8/8	6/6	6/6	6/6	5/5	23/23
Race, n (%)						
White	5 (62.5)	4 (66.7)	3 (50.0)	5 (83.3)	4 (80.0)	16 (69.6)
Black or African American	3 (37.5)	2 (33.3)	3 (50.0)	1 (16.7)	1 (20.0)	7 (30.4)
Ethnic group, n (%)						
Hispanic or Latino	8 (100)	6 (100)	5 (83.3)	6 (100)	5 (100)	22 (95.7)
Not Hispanic or Latino	0	0	1 (16.7)	0	0	1 (4.3)
Age (years)						
Mean (SD)	35.50 (10.20)	44.70 (8.10)	43.60 (9.50)	39.70 (11.20)	35.80 (11.80)	41.10 (10.10)
Median	33.70	45.80	45.60	37.80	34.80	42.20
Minimum, maximum	22.5, 52.6	31.0, 53.0	30.9, 53.0	28.0, 53.0	24.0, 47.9	24.0, 53.0
Height (cm)						
Mean (SD)	172.50 (6.30)	171.00 (6.30)	174.60 (10.70)	176.80 (9.10)	169.80 (5.80)	173.20 (8.30)
Median	173.50	168.00	171.50	181.00	170.00	171.00
Minimum, maximum	160.0, 179.0	166.0, 183.0	166.0, 195.0	163.0, 184.0	161.0, 175.0	161.0, 195.0
Weight (kg)						
Mean (SD)	81.70 (7.50)	84.30 (9.30)	84.50 (8.90)	84.40 (8.70)	73.80 (18.30)	82.10 (11.60)
Median	79.20	83.50	83.40	82.70	75.80	83.00
Minimum, maximum	72.7, 95.8	72.5, 99.8	70.8, 95.2	72.7, 94.7	52.8, 92.0	52.8, 99.8
Body mass index (kg/m^2)						
Mean (SD)	27.50 (1.90)	28.80 (1.60)	27.70 (2.40)	27.00 (3.80)	25.20 (5.00)	27.20 (3.40)
Median	26.70	29.50	28.50	28.70	25.70	29.20
Minimum, maximum	25.6, 30.0	25.8, 29.9	24.3, 30.0	21.0, 30.0	18.6, 29.9	18.6, 30.0

*Because of the IgG lower limit of normal (LLN) stopping rule, one individual was not enrolled into the 30 mg/kg cohort.

preadministration levels in the 1, 3, and 10 mg/kg groups. All individuals treated with SYNT001 (1, 3, or 10 mg/kg) maintained IgG levels above the LLN throughout the study. In contrast, four of five individuals in the SYNT001 30 mg/kg dose group exhibited IgG levels below the LLN by day 5. Therefore, the sixth individual was not enrolled in the SYNT001 30 mg/kg cohort. Reductions in total circulating IgG in the 30 mg/kg group were also reversible as evidenced by their median return to within −27.33% (IQR, −29.87 to −27.11%) below baseline by day 28 after dosing.

Table 4. TEAEs by preferred term—safety population. Note that each individual was only counted once per preferred term.

Preferred term	Vehicle (n = 8)	SYNT001 (1 mg/kg) (n = 6)	SYNT001 (3 mg/kg) (n = 6)	SYNT001 (10 mg/kg) (n = 6)	SYNT001 (30 mg/kg) (n = 5)	Pooled SYNT001 (n = 23)
Individuals with ≥1 TEAE, n (%)	1 (12.5)	0	0	3 (50.0)	5 (100)	8 (34.8)
Headache	0	0	0	3 (50.0)	5 (100)	8 (34.8)
Chills	1 (12.5)	0	0	0	1 (20.0)	1 (4.3)
Presyncope	0	0	0	1 (16.7)	0	1 (4.3)
Fatigue	0	0	0	1 (16.7)	0	1 (4.3)
Pyrexia	0	0	0	1 (16.7)	0	1 (4.3)
Abdominal pain	0	0	0	0	1 (20.0)	1 (4.3)
Diarrhea	0	0	0	0	1 (20.0)	1 (4.3)
Nausea	0	0	0	0	1 (20.0)	1 (4.3)
Arthralgia	0	0	0	1 (16.7)	0	1 (4.3)
Muscular weakness	0	0	0	1 (16.7)	0	1 (4.3)
Myalgia	0	0	0	1 (16.7)	0	1 (4.3)
Lacrimation increased	0	0	0	1 (16.7)	0	1 (4.3)
Decreased appetite	0	0	0	0	1 (20.0)	1 (4.3)
Rhinorrhea	0	0	0	1 (16.7)	0	1 (4.3)

Table 5. Summary of PK parameter estimates in healthy individuals treated with single dose of SYNT001. $AUC_{(0-t)}$, AUC from time 0 to the last time point with a concentration level ≥ limit of quantitation; λ_Z, terminal elimination rate constant; V_d, apparent volume of distribution during terminal phase after extravascular administration.

Dose group	Parameter	C_{max} (ng/ml)	T_{max} (hours)	$AUC_{(0-24h)}$ (hours·ng/ml)	$AUC_{(0-t)}$ (hours·ng/ml)	$AUC_{(0-inf)}$ (hours·ng/ml)	λ_Z (1/hours)	$T_{1/2}$ (hours)	V_d (ml/kg)	C_L (ml/hour/kg)
1 mg/kg*	n	6	6	6	6	1	1	1	1	1
	Mean	18084.083		29794.634	29296.491	52632.931	1.090	0.636	17.435	19.000
	SD	5745.119		11827.081	11903.121					
	Median	16119.85	0.080	25930.50	25279.30					
3 mg/kg	n	6	6	6	6	6	6	6	6	6
	Mean	73416.550		394468.202	392122.944	394584.153	0.529	1.407	15.395	7.877
	SD	9179.148		80783.509	80447.160	81092.936	0.163	0.398	2.755	1.626
	Median	76778.35	0.080	395961.27	392572.86	396103.65	0.50	1.39	15.69	7.60
10 mg/kg	n	6	6	6	6	6	6	6	6	6
	Mean	299330.000		3286692.228	3283820.283	3462471.993	0.140	5.297	23.022	3.011
	SD	65568.274		709349.625	708586.918	733659.101	0.045	1.441	8.133	0.708
	Median	304908.00	0.080	3281142.00	3279597.38	3466938.84	0.13	5.32	21.47	2.89
30 mg/kg	n	5	5	5	5	5	5	5	5	5
	Mean	912819.600		12227632.060	15752080.833	16556146.477	0.131	7.794	18.755	1.945
	SD	162351.117		2399425.464	3838139.142	5091946.878	0.081	6.234	9.157	0.553
	Median	955306.00	0.080	11977325.16	14730835.80	14805600.06	0.12	5.56	16.26	2.03

*In the 1 mg/kg dose group, only one individual had ≥3 sample points after T_{max}; thus, AUC_{0-inf}, $t_{1/2}$, V_d, C_L, and λ_Z were only computed for that one individual.

We observed reductions across all four IgG subtypes with the 30 mg/kg dose group displaying the lowest levels (Fig. 3C). Median levels remained above the LLN throughout the 28-day postdose period at all dose levels. The greatest median decreases were in the 30 mg/kg dose group for IgG3 (−68.29%; IQR, −71.83 to −61.38%) with lesser reductions of IgG1 (−51.62%; IQR, −52.62 to −49.80%), IgG2 (−36.92%; IQR, −39.81 to −33.56%), and IgG4 (−42.86%; IQR. −42.86 to −41.935%) (Fig. 3C and fig. S3, B to E). The level of IgG subtypes returned to
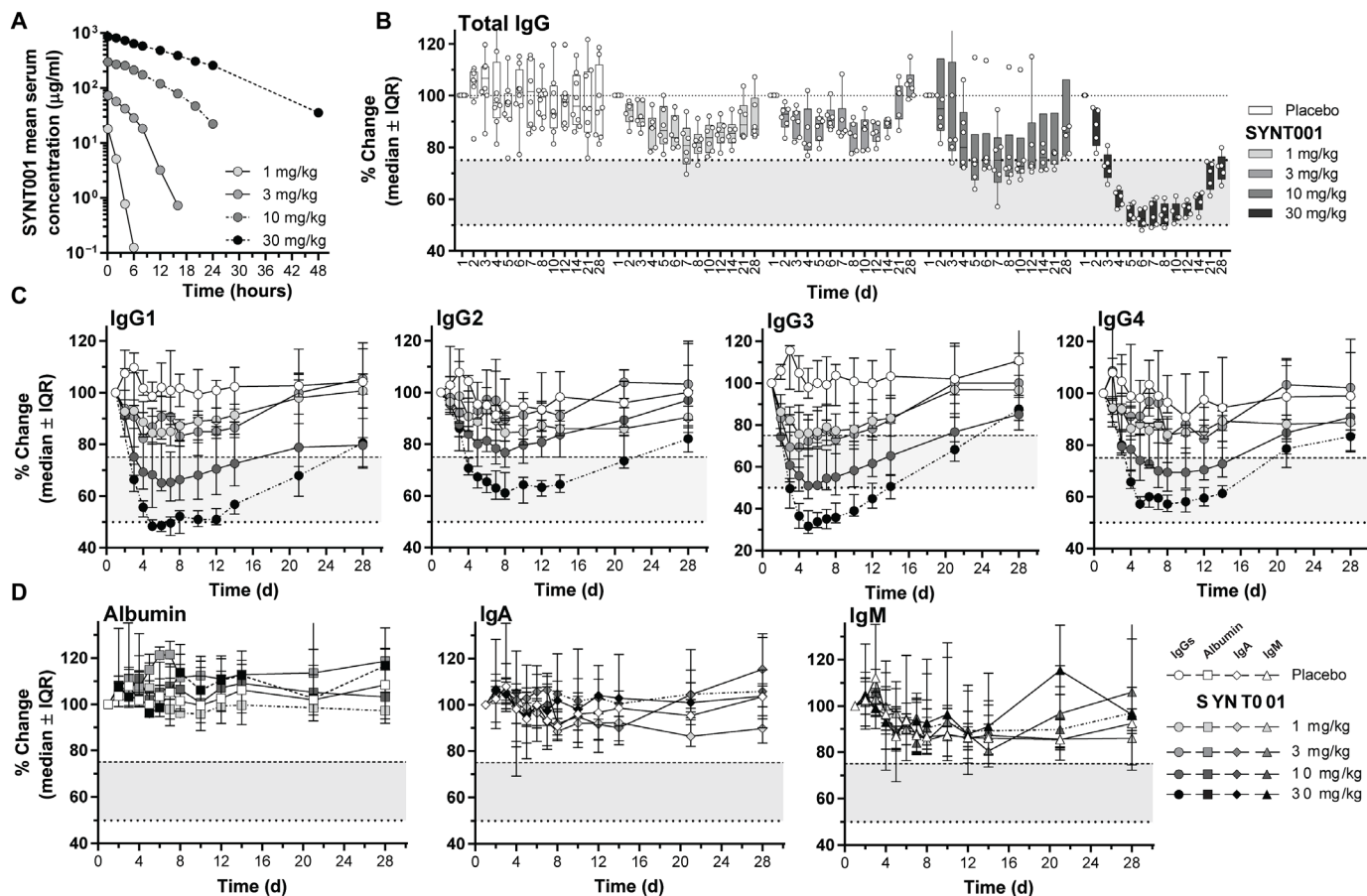
Fig. 3. PK and PD of single-dose SYNT001 administration in healthy individuals. (**A**) Mean SYNT001 serum concentration time plots for all SYNT001 cohorts. Median percentage change in (**B**) total circulating IgG and (**C**) IgG1, IgG2, IgG3, and IgG4 for all SYNT001 cohorts. Reference ranges for each subtype were as follows: IgG1, 240 to 1118 mg/dl; IgG2, 124 to 549 mg/dl; IgG3, 21 to 134 md/dl; IgG4. 1 to 123 mg/dl. (**D**) Median percentage change in circulating albumin, IgA, and IgM for all SYNT001 cohorts. Baseline is defined as predose day 1 concentration. Median ± interquartile range (IQR) are shown (*n* = 8 for placebo, *n* = 6 for 1, 3, and 10 mg/kg, and *n* = 5 for 30 mg/kg groups). In (B), symbols represent individual data points from each individual volunteer. Fine dotted lines correspond to baseline level. Bold dotted lines correspond to 75 and 50% change levels with shaded area in between. (B and C) MMRM modeling indicated statistically significant (*P* < 0.05) differences of IgG levels compared to placebo in the 1 mg/kg (days 2 to 14), 3 mg/kg (days 2 to 10), 10 mg/kg (days 2 to 14), and 30 mg/kg (days 2 to 21) dose groups.

within 25% of baseline levels by day 28 in all dose groups. Three individuals in the 30 mg/kg dose group experienced IgG3 levels below the LLN between days 4 and 14. No significant changes were observed in the levels of albumin, IgA, and IgM (Fig. 3D and fig. S3, F to H).

Immunogenicity

We screened a total of 93 human serum samples from 31 enrolled individuals for binding ADAs at days 1, 14, and 28 of the study. Six of 93 samples (6.5%) that were derived from 5 of 31 individuals (16.1%) were confirmed to be positive. Two individuals in the 1 mg/kg dose group (on days 14 and 28), one individual in the 3 mg/kg dose group (on days 14 and 28), and two individuals in the 10 mg/kg dose group (both on day 14 only) tested positive. The ADA titers detected were low and were not observed to be neutralizing. Thus, we detected a low frequency of transient, low-titer, and non-neutralizing ADAs.

Immune effects

Healthy human individuals maintain low levels of CICs, which permitted assessment of SYNT001 effect on their levels (*35*). CICs were

quantified by an enzyme-linked immunosorbent assay (ELISA), which detects C1q bound, and thus complement-fixed, IgG antibodies. At baseline, the median CIC levels for all individuals was 2.6 μg/ml (IQR, 1.90 to 3.90), which was within the normal range of the laboratory reference (0 to 3.9 μg/ml). The samples for the 1 mg/kg dose group and data beyond day 12 for the 3, 10, and 30 mg/kg dose groups were not available for evaluation due to sample integrity issues. The administration of SYNT001, but not placebo, resulted in a dose-dependent decrease in CICs (Fig. 4A). The nadir in CIC levels occurred 7 days after SYNT001 administration declining by 18.98% (IQR, 25 to 18.18%), 29.41% (IQR, 31.58 to 25.71%), and 48.39% (IQR, 55.56 to 40.91%) from baseline levels in the 3, 10, and 30 mg/kg groups, respectively. Overall, the reductions persisted for up to 10 days after a single administration of SYNT001.

Cytokine production from human monocyte-derived DC in response to IgG ICs has been shown to be dependent on FcRn (*23*). To further validate the effects of SYNT001 on CIC, we established a novel in vitro assay by exposing heparinized human whole blood from healthy donors to hIgG1 ICs. Although hIgG1^WT ICs induced robust secretion of tumor necrosis factor–α (TNFα) and interleukin-6 (IL-6)
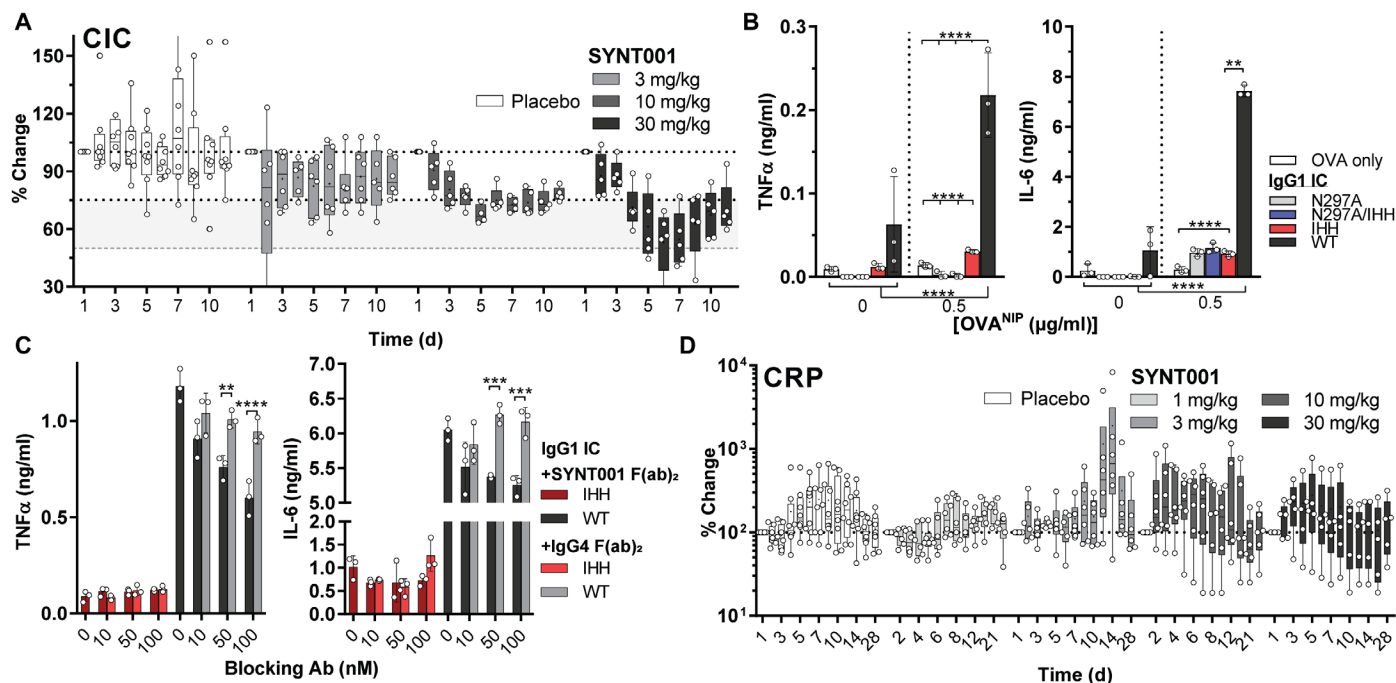
Fig. 4. Effect of FcRn blockade by SYNT001 on immune responses in healthy individuals. (**A**) Median percentage change in total CICs for placebo or 3, 10, and 30 mg/kg SYNT001 cohorts. Median ± IQR is shown with symbols representing actual data points from each individual volunteer ($n = 8$ for placebo, $n = 6$ for 3 and 10 mg/kg, and $n = 5$ for 30 mg/kg groups). FcRn-dependent induction of inflammatory responses to IgG ICs in human whole blood. (**B**) Analysis of TNFα and IL-6 secretion by IgG IC–stimulated human cells in heparinized blood obtained from representative healthy human volunteer 24 hours after stimulation. Means ± SEM is depicted with open circles representing actual data points. (**C**) SYNT001 inhibits FcRn-dependent IgG IC–induced innate immune response. Analysis of TNFα secretion by IgG IC–stimulated human leukocytes in presence of increasing doses of F(ab)$_2$ SYNT001 or F(ab)$_2$ IgG4 isotype controls from representative healthy human volunteer 24 hours after stimulation. Means ± SEM is depicted with open circles representing individual data points. Ab, antibody. (**D**) Median percentage change in C-reactive protein (CRP) levels for all SYNT001 cohorts. Baseline is defined as predose day 1 concentration. Median ± IQR is shown with symbols representing data points from each individual volunteer ($n = 8$ for vehicle, $n = 6$ for 1, 3, and 10 mg/kg, and $n = 5$ for 30 mg/kg groups). (A) Statistically significant decrease in CIC levels ($P < 0.05$) in the dose group (3 mg/kg) (days 2 to 7) and in the 10 and 30 mg/kg dose groups (days 2 to 10) compared to placebo were determined by MMRM modeling. (B) **$P = 0.0075$, ****$P < 0.0001$ by two-way ANOVA with Fisher's LSD post hoc test; (C) **$P < 0.01$, ***$P < 0.0007$, ****$P < 0.0001$ by two-way ANOVA with Fisher's LSD post hoc test. In vitro experiments were repeated at least twice with (B) three or (C) two different donors of which only one is shown.

within 24 hours, ICs composed of IgG engineered variants that are unable to bind FcRn (IgG1^{IHH}), FcγR (hIgG1^{N297A}), or both (hIgG1$^{N297A/IHH}$) stimulated significantly less secretion (Fig. 4B) (*22*, *24*, *36*). Thus, FcRn controls the induction of inflammatory cytokines by primary human peripheral blood cells in response to IgG ICs even in the context of FcγR engagement. We therefore next examined the ability of SYNT001 to inhibit IgG IC–induced innate immune responses. To eliminate the nonspecific effects of the human Fc fragment in this assay, we used F(ab′)$_2$ fragments and observed that SYNT001 F(ab′)$_2$ fragments, but not F(ab′)$_2$ fragments of an isotype control, inhibited TNFα and IL-6 secretion in a dose-dependent manner (Fig. 4C). SYNT001 can thus inhibit FcRn-mediated protection of CICs and impede IgG IC activation of FcRn-mediated innate cytokine production. Last, consistent with the absence of effects on circulating blood counts or evidence of significant safety findings, we did not observe increases in serum C-reactive protein (Fig. 4D) or a panel of cytokines (fig. S4, A to L) in any of the dose groups over time relative to that observed in the placebo treated individuals in this single ascending dose study.

DISCUSSION

This report describes the generation of SYNT001, a humanized monoclonal IgG4 antibody that blocks IgG binding to hFcRn and

its characterization in humanized mice, NHPs, and in a first-in-human phase 1a clinical study. SYNT001 was well tolerated in NHPs and humans, and its administration reduced the serum concentrations of total IgG. Following a single dose of 30 mg/kg in humans, we observed decreases in total IgG and IgG1, IgG2, and IgG4 subclasses by approximately 40 to 50%, while IgG3 was uniquely susceptible with a reduction of up to 70%. The extent of IgG depletion achieved was to levels previously correlated with clinical responses observed in individuals who have undergone immunoadsorption or plasmapheresis for the treatment of autoimmune diseases caused by pathogenic autoantibodies (*37*–*39*). In addition, the level of total IgG reduction after a single dose of SYNT001 in humans was similar to that observed in NHPs. In light of the 70% decline in total circulating IgG levels observed in the 100 mg/kg SYNT001 primate study group, we expect comparable total serum IgG depletion effects in humans upon higher or repetitive SYNT001 dose administration. Together with initial results from a phase 1b study in patients with pemphigus that demonstrate the ability of SYNT001 to decrease anti-desmoglein antibody levels and IgG ICs in association with clinical responses (*40*), these studies support the potential utility of SYNT001 in the treatment of autoimmune diseases by decreasing pathogenic autoantibody levels.

As predicted by studies in radiation bone marrow chimeric mice whereby absence of FcRn expression in cells of hematopoietic origin

resulted in faster clearance of IgG ICs (22), SYNT001 also caused a significant dose-dependent reduction of CIC in humans. Our studies therefore uniquely reveal a well-tolerated pharmacologic intervention that can remove IgG ICs from the circulation. Removal of CICs is noteworthy as it has heretofore only been achieved through invasive interventions such as immunoadsorption or plasmapheresis (41). We also observed that FcRn blockade with SYNT001 inhibited the ability of IgG ICs to induce secretion of innate inflammatory cytokines by human peripheral blood leukocytes when examined ex vivo. Together with the ability of SYNT001 to disable IgG IC engagement of Ag presentation pathways associated with activation of CD4+ and CD8+ T cells by mouse APCs expressing hFcRn as we observed, these results support the role of FcRn in enabling a wide variety of IgG IC–mediated inflammatory pathways. Hence, these results have broad implications and suggest that SYNT001 may be useful in clinical scenarios where IgG ICs are directly causing disease through deposition in tissues (e.g., IC nephritis) (42), through induction of phagocytosis and thrombosis (e.g., warm autoimmune hemolytic anemia and heparin-induced thrombocytopenia) (15, 43), or indirectly through activation of innate and adaptive immune responses (e.g., inflammatory bowel disease and rheumatoid arthritis) (7, 44).

SYNT001 reduction of circulating monomeric IgG and CIC was observed to be rapid with a nadir occurring within 5 to 6 days after dosing. Moreover, these effects were durable in that they were evident for at least a month after a single dose of drug administration yet reversible and returned to within 25% of the baseline levels by day 28 in the highest dose group. The activities of FcRn that relate to recycling and protection of IgG on the one hand or promoting the persistence and immune properties of IgG ICs on the other are likely derived from the distinct properties of the cell types that express FcRn and its functional localization within them. This suggests that SYNT001 was interacting with FcRn in multiple cell–associated compartments. The main FcRn functional fraction involved in protecting IgG and albumin from degradation is intracellular and contained primarily within early and recycling endosomes of various cell types after fluid phase endocytosis of internalized ligands (18, 19, 45). Consistent with this, cells of endothelial and epithelial origin are solely involved in the protection and transport of IgG (46) and predominantly express FcRn in intracellular organelles (29). Monomeric IgG is equivalently protected by FcRn in myeloid cells, which are also the main cell type involved in IgG IC interactions due to their expression of classical FcγR (13, 20–22). Previous studies have shown that large internalized IgG ICs are retained by FcRn in late endosomes and lysosomal-associated membrane protein 1 (LAMP-1+) organelles of APCs where they have been demonstrated to be important for FcRn-mediated immune responses (22). In addition, most of the circulating human leukocytes such as neutrophils, monocytes, and DCs uniquely express significant levels of FcRn on the cell surface as we show here. Although the functional role of FcRn in this locale is unknown, previous studies have shown that phagocytosis of IgG-opsonized particles is perturbed in absence of FcRn (15). Together, these observations suggest that inhibition of FcRn regulation of IgG levels and responses to IgG ICs involve entry of therapeutic agents into multiple cell–associated compartments within parenchymal and hematopoietic cell types.

A critical issue concerning anti-FcRn therapy is whether antibodies to FcRn cause receptor degradation. We show here that administration of SYNT001 to NHPs was associated with transient decreases in monocyte surface FcRn expression suggesting receptor internalization and a PK profile characteristic of target-mediated disposition, without major alterations in the total levels of FcRn. At any administered dose, SYNT001 did not cause a decrease in FcRn's second ligand, albumin. These data thus argue against receptor degradation upon treatment with SYNT001.

The results of our studies are distinguished in several regards with respect to other recent phase 1 clinical studies targeting FcRn (25–27). First, using SYNT001, we demonstrate that FcRn blockade can force the destruction and inhibit the immunologic activities of IgG ICs in humans. This importantly suggests that FcRn promotes inflammation through binding IgG ICs, which SYNT001 inhibits. Second, SYNT001 blockade of FcRn also had no effect on albumin levels in the circulation, which is of interest, as transient reductions of albumin have been observed in two anti-FcRn antibody clinical trials (25, 27); in at least two cases (25, 47), it has been suggested to be due to steric hindrance by the therapeutic antibody. One possibility for the latter is that SYNT001 occupies the FcRn α chain and β2m interface in a manner that is similar to native Fc binding and may mirror physiologic interactions. In summary, the results of these studies predict that FcRn blockade using SYNT001 has the potential to treat a variety of inflammatory and autoimmune conditions, making it a promising therapeutic agent in reversing the effects of pathogenic IgG and IgG ICs.

MATERIALS AND METHODS

Clinical study design

Study of SYNT001 was performed in a phase 1a, single-center (Clinical Pharmacology of Miami, Miami, FL), double-blind, randomized (6:2), placebo-controlled, single ascending dose study of SYNT001 in healthy male individuals (www.clinicaltrials.gov; identifier NCT03643627). The study was approved by IntegReview IRB (Austin, TX), and all individuals provided written informed consent. This study was designed to assess the safety, tolerability, PK, and PD of SYNT001. Five sequential cohorts were to receive single doses of 1, 3, 10, 30, and 60 mg/kg of SYNT001 or placebo (dextrose 5% in water) administered as a 250-ml intravenous infusion over 1 hour. Individuals were dosed on day 1 and followed for 27 days after dosing (to day 28). Individuals remained at the clinic for 48 hours following the end of the infusion.

To avoid unnecessary hypogammaglobulinemia in healthy individuals, the study included a stopping rule: If ≥1 individual exhibited serum total IgG levels below the reference lab's LLN (768 mg/dl) at any time following SYNT001 dosing, then no further dosing would occur. Thus, eligible individuals were required to have total IgG levels greater than or equal to the midpoint of the reference lab's normal range (1200 mg/dl) at entry. Up to 40 individuals were planned for enrollment. As the study stopping rule regarding total IgG levels was met after enrolling seven of a planned total of eight individuals in cohort 4 (30 mg/kg), 31 total individuals were enrolled in the study. No individuals were dosed in cohort 5 at 60 mg/kg. PK, PD, and safety evaluations were performed during each individual's stay in the clinic and upon their return to the clinic on days 4 to 8, 10, 12, 14, 21, and 28. The National Cancer Institute Common Terminology Criteria for Adverse Events (version 4.03) was used for grading clinical and laboratory toxicities.

PK assessments

Testing of healthy individuals sera for PK analysis consisted of the validated Competitive Binding Electrochemiluminescence (ECL) ELISA

(MPI Research Laboratories, Mattawan, MI). Plates were coated with anti-hFcRn, followed by recombinant hFcRn to capture SYNT001. SULFO-TAG–labeled SYNT001 at a set concentration was combined with samples to allow binding of FcRn for quantification of samples in a competitive format. MSD (Meso Scale Discovery) Read Buffer T was added before analysis on an MSD Sector Imager. PK data were analyzed using a noncompartmental analysis method as implemented in Phoenix WinNonlin v6.4 (Certara, Princeton, NJ).

PD assessments of IgG, IgG subtypes, IgA, IgM, albumin, C-reactive protein, and CICs

Serum samples were assessed by means of immunonephelometry on the BN II nephelometric analyzer (Siemens, Munich, Germany) using Human IgG (NAS IGG, ASAS09, Siemens), IgA (NAS IGA. OSAR09, Siemens), IgM (NAS IGM, OSAT09, Siemens), Human IgG Subclass Liquid (LK001.TB, NK006.TB, NK007.TB, LK008.TB, and LK009.TB, Siemens), Albumin (NAS ALB, OSAL11, Siemens), or C-reactive protein (N CardioPhase, OQIY21, Siemens) reagents according to the manufacturer's instructions at Charles River Laboratories (Paw Paw, MI). CICs were assessed by a standard sandwich ELISA, MicroVue CIC-C1q EIA Kit (A001, Quidel), which detects C1q-associated IgG aggregates according to the manufacturer's instructions. Serum or plasma samples were diluted 1:50.

Measurement of ADA

A total of three serum samples (5 ml each; total of 15 ml) were collected for immunogenicity analyses on days 1 (before dose), 14, and 28. The ADA assay method was a sandwich MSD ECL ELISA (Rockville, MD). MSD plates were coated with streptavidin and then captured with biotin-labeled SYNT001. Serum from all individuals participating in the study or additional controls was then added, followed by detection with SULFO-TAG–labeled SYNT001. During method validation, it was determined that the screening assay cut point factor was 3.34 optical density units based on a 5% false-positive rate with a 90% confidence level. Any test articles that were greater than or equal to the screening cut point then underwent confirmatory testing. The confirmatory assay cut point was determined to be 67.57% signal inhibition. Any confirmatory assay test articles that were greater than or equal to the confirmatory assay cut point were then tested for titer to determine the level of anti-SYNT001–specific antibodies present. Titer was a numeric value calculated as reciprocal of a dilution factor.

The neutralizing antibody assay was designed to measure the ability of anti-SYNT001 antibodies to inhibit test article binding to FcRn. For neutralizing steps, plates were coated with anti-FcRn and then SYNT001 and test articles or controls, followed by hFcRn. These neutralizing step incubations occurred at neutral pH. The detection steps consisted of adding biotin-labeled hIgG1, followed by streptavidin–horseradish peroxidase and 3,3′,5,5′-tetramethylbenzidine ELISA substrate. These detection step incubations occurred at pH 6.0 and were separated from capture pH to avoid competition with serum IgGs. During method validation, the neutralizing antibody assay cut point factor was determined to be 1.39 optical density units based on a 5% false-positive rate with a 90% confidence level.

Measurement of serum cytokines

Serum cytokines were measured by a contractor, ARUP Laboratories (Salt Lake City, UT) using the Luminex 200 analyzer (Thermo Fisher Scientific, Waltham, MA) and Luminex 200 multi-analyte profiling technology. Custom made, clinically validated, laboratory-developed test cytokine panel (0051394, ARUP Laboratories) consisted of 11 cytokines (IL-1β, IL-2, IL-4, IL-5, IL-6, IL-8, IL-10, IL-12, IL-13, TNFα, and IFN-γ) and one soluble cytokine receptor (sIL-2Rα, sCD25) with a lower detection limit of 5 pg/ml. This test was developed and its performance characteristics determined by ARUP Laboratories.

Statistical methods

Prism 7.04 (GraphPad Software Inc., La Jolla, CA) was used for statistical analysis. Statistical comparisons between two groups were made by Student's t test. For three or more groups with two parameters, two-way analysis of variance (ANOVA) was used. Post hoc analysis to detect differences between treatment groups was performed by uncorrected Fisher's least significant difference (LSD) test. In addition, mixed-effects model repeated-measures modeling analysis was used using SAS v9.4 (Cary, NC) to evaluate statistical significance in NHP and human studies. A two-sided probability (P) of α error of less than 0.05 was considered significant.

SUPPLEMENTARY MATERIALS

Supplementary material for this article is available at http://advances.sciencemag.org/cgi/content/full/5/12/aax9586/DC1

Fig. S1. Characterization of SYNT001.
Fig. S2. The immunologic effects of repeated-dose SYNT001 administration in cynomolgus monkeys.
Fig. S3. PD of single-dose SYNT001 administration in healthy human individuals.
Fig. S4. Effect of FcRn-blockade by SYNT001 on immune responses in healthy individuals.
Table S1. SYNT001-FcRn:β₂m crystal structure data collection and refinement statistics (Protein Data Bank ID: 6NHA).
References (48–60)

View/request a protocol for this paper from *Bio-protocol*.

REFERENCES AND NOTES

1. R. J. Ludwig, K. Vanhoorelbeke, F. Leypoldt, Z. Kaya, K. Bieber, S. M. McLachlan, L. Komorowski, J. Luo, O. Cabral-Marques, C. M. Hammers, J. M. Lindstrom, P. Lamprecht, A. Fischer, G. Riemekasten, C. Tersteeg, P. Sondermann, B. Rapoport, K. P. Wandinger, C. Probst, A. el Beidaq, E. Schmidt, A. Verkman, R. A. Manz, F. Nimmerjahn, Mechanisms of autoantibody-induced pathology. *Front. Immunol.* **8**, 603 (2017).

2. J. Suurmond, B. Diamond, Autoantibodies in systemic autoimmune diseases: Specificity and pathogenicity. *J. Clin. Invest.* **125**, 2194–2202 (2015).

3. A. Sesarman, A. G. Sitaru, F. Olaru, D. Zillikens, C. Sitaru, Neonatal Fc receptor deficiency protects from tissue injury in experimental epidermolysis bullosa acquisita. *J. Mol. Med.* **86**, 951–959 (2008).

4. L. Liu, A. M. Garcia, H. Santoro, Y. Zhang, K. McDonnell, A. Dumont, A. Bitonti, Amelioration of experimental autoimmune myasthenia gravis in rats by neonatal FcR blockade. *J. Immunol.* **178**, 5390–5398 (2007).

5. A. R. Mezo, K. A. McDonnell, C. A. T. Hehir, S. C. Low, V. J. Palombella, J. M. Stattel, G. D. Kamphaus, C. Fraley, Y. Zhang, J. A. Dumont, A. J. Bitonti, Reduction of IgG in nonhuman primates by a peptide antagonist of the neonatal Fc receptor FcRn. *Proc. Natl. Acad. Sci. U.S.A.* **105**, 2337–2342 (2008).

6. N. Li, M. Zhao, J. Hilario-Vargas, P. Prisayanh, S. Warren, L. A. Diaz, D. C. Roopenian, Z. Liu, Complete FcRn dependence for intravenous Ig therapy in autoimmune skin blistering diseases. *J. Clin. Invest.* **115**, 3440–3450 (2005).

7. S. Akilesh, S. Petkova, T. J. Sproule, D. J. Shaffer, G. J. Christianson, D. Roopenian, The MHC class I–like Fc receptor promotes humorally mediated autoimmune disease. *J. Clin. Invest.* **113**, 1328–1333 (2004).

8. M. Pyzik, K. M. K. Sand, J. J. Hubbard, J. T. Andersen, I. Sandlie, R. S. Blumberg, The neonatal Fc receptor (FcRn): A misnomer? *Front. Immunol.* **10**, 1540 (2019).

9. E. J. Israel, S. Taylor, Z. Wu, E. Mizoguchi, R. S. Blumberg, A. Bhan, N. E. Simister, Expression of the neonatal Fc receptor, FcRn, on human intestinal epithelial cells. *Immunology* **92**, 69–74 (1997).

10. J. Borvak, J. Richardson, C. Medesan, F. Antohe, C. Radu, M. Simionescu, V. Ghetie, E. S. Ward, Functional expression of the MHC class I–related receptor, FcRn, in endothelial cells of mice. *Int. Immunol.* **10**, 1289–1298 (1998).

11. M. Pyzik, T. Rath, T. T. Kuo, S. Win, K. Baker, J. J. Hubbard, R. Grenha, A. Gandhi, T. D. Krämer, A. R. Mezo, Z. S. Taylor, K. McDonnell, V. Nienaber, J. T. Andersen, A. Mizoguchi, L. Blumberg, S. Purohit, S. D. Jones, G. Christianson, W. I. Lencer, I. Sandlie, N. Kaplowitz, D. C. Roopenian, R. S. Blumberg, Hepatic FcRn regulates albumin homeostasis and susceptibility to liver injury. *Proc. Natl. Acad. Sci. U.S.A.* **114**, E2862–E2871 (2017).

12. X. Zhu, G. Meng, B. L. Dickinson, X. Li, E. Mizoguchi, L. Miao, Y. Wang, C. Robert, B. Wu, P. D. Smith, W. I. Lencer, R. S. Blumberg, MHC class I-related neonatal Fc receptor for IgG is functionally expressed in monocytes, intestinal macrophages, and dendritic cells. *J. Immunol.* **166**, 3266–3276 (2001).

13. S. Akilesh, G. J. Christianson, D. C. Roopenian, A. S. Shaw, Neonatal FcR expression in bone marrow-derived cells functions to protect serum IgG from catabolism. *J. Immunol.* **179**, 4580–4588 (2007).

14. W. Mi, S. Wanjie, S. T. Lo, Z. Gan, B. Pickl-Herk, R. J. Ober, E. S. Ward, Targeting the neonatal Fc receptor for antigen delivery using engineered Fc fragments. *J. Immunol.* **181**, 7550–7561 (2008).

15. G. Vidarsson, A. M. Stemerding, N. M. Stapleton, S. E. Spliethoff, H. Janssen, F. E. Rebers, M. de Haas, J. G. van de Winkel, FcRn: An IgG receptor on phagocytes with a novel role in phagocytosis. *Blood* **108**, 3573–3579 (2006).

16. C. Chaudhury, C. L. Brooks, D. C. Carter, J. M. Robinson, C. L. Anderson, Albumin binding to FcRn: Distinct from the FcRn-IgG interaction. *Biochemistry* **45**, 4983–4990 (2006).

17. Z. Gan, S. Ram, C. Vaccaro, R. J. Ober, E. S. Ward, Analyses of the recycling receptor, FcRn, in live cells reveal novel pathways for lysosomal delivery. *Traffic* **10**, 600–614 (2009).

18. P. Prabhat, Z. Gan, J. Chao, S. Ram, C. Vaccaro, S. Gibbons, R. J. Ober, E. S. Ward, Elucidation of intracellular recycling pathways leading to exocytosis of the Fc receptor, FcRn, by using multifocal plane microscopy. *Proc. Natl. Acad. Sci. U.S.A.* **104**, 5889–5894 (2007).

19. E. G. W. Schmidt, M. L. Hvam, F. Antunes, J. Cameron, D. Viuff, B. Andersen, N. N. Kristensen, K. A. Howard, Direct demonstration of a neonatal Fc receptor (FcRn)–driven endosomal sorting pathway for cellular recycling of albumin. *J. Biol. Chem.* **292**, 13312–13322 (2017).

20. W. F. Richter, G. J. Christianson, N. Frances, H. P. Grimm, G. Proetzel, D. C. Roopenian, Hematopoietic cells as site of first-pass catabolism after subcutaneous dosing and contributors to systemic clearance of a monoclonal antibody in mice. *MAbs*, 803–813 (2018).

21. D. K. Challa, X. Wang, H. P. Montoyo, R. Velmurugan, R. J. Ober, E. S. Ward, Neonatal Fc receptor expression in macrophages is indispensable for IgG homeostasis. *MAbs* **11**, 848–860 (2019).

22. S. W. Qiao, K. Kobayashi, F. E. Johansen, L. M. Sollid, J. T. Andersen, E. Milford, D. C. Roopenian, W. I. Lencer, R. S. Blumberg, Dependence of antibody-mediated presentation of antigen on FcRn. *Proc. Natl. Acad. Sci. U.S.A.* **105**, 9337–9342 (2008).

23. K. Baker, T. Rath, M. B. Flak, J. C. Arthur, Z. Chen, J. N. Glickman, I. Zlobec, E. Karamitopoulou, M. D. Stachler, R. D. Odze, W. I. Lencer, C. Jobin, R. S. Blumberg, Neonatal Fc receptor expression in dendritic cells mediates protective immunity against colorectal cancer. *Immunity* **39**, 1095–1107 (2013).

24. K. Baker, S. W. Qiao, T. T. Kuo, V. G. Aveson, B. Platzer, J. T. Andersen, I. Sandlie, Z. Chen, C. de Haar, W. I. Lencer, E. Fiebiger, R. S. Blumberg, Neonatal Fc receptor for IgG (FcRn) regulates cross-presentation of IgG immune complexes by CD8⁻CD11b⁺ dendritic cells. *Proc. Natl. Acad. Sci. U.S.A.* **108**, 9927–9932 (2011).

25. P. Kiessling, R. Lledo-Garcia, S. Watanabe, G. Langdon, D. Tran, M. Bari, L. Christodoulou, E. Jones, G. Price, B. Smith, F. Brennan, I. White, S. Jolles, The FcRn inhibitor rozanolixizumab reduces human serum IgG concentration: A randomized phase 1 study. *Sci. Transl. Med.* **9**, eaan1208 (2017).

26. P. Ulrichts, A. Guglietta, T. Dreier, T. van Bragt, V. Hanssens, E. Hofman, B. Vankerckhoven, P. Verheesen, N. Ongenae, V. Lykhopiy, F. J. Enriquez, J. H. Cho, R. J. Ober, E. S. Ward, H. de Haard, N. Leupin, Neonatal Fc receptor antagonist efgartigimod safely and sustainably reduces IgGs in humans. *J. Clin. Invest.* **128**, 4372–4386 (2018).

27. L. Ling, J. L. Hillson, R. G. Tiessen, T. Bosje, M. P. van Iersel, D. J. Nix, L. Markowitz, N. A. Cilfone, J. Duffner, J. B. Streisand, A. M. Manning, S. Arroyo, M281, an anti-FcRn antibody: Pharmacodynamics, pharmacokinetics, and safety across the full range of IgG reduction in a first-in-human study. *Clin. Pharmacol. Ther.* **105**, 1031–1039 (2018).

28. C. Cianga, P. Cianga, P. Plamadeala, C. Amalinei, Nonclassical major histocompatibility complex I-like Fc neonatal receptor (FcRn) expression in neonatal human tissues. *Hum. Immunol.* **72**, 1176–1187 (2011).

29. S. Latvala, B. Jacobsen, M. B. Otteneder, A. Herrmann, S. Kronenberg, Distribution of FcRn across species and tissues. *J. Histochem. Cytochem.* **65**, 321–333 (2017).

30. C. Stein, L. Kling, G. Proetzel, D. C. Roopenian, M. H. de Angelis, E. Wolf, B. Rathkolb, Clinical chemistry of human FcRn transgenic mice. *Mamm. Genome* **23**, 259–269 (2011).

31. S. B. Petkova, S. Akilesh, T. J. Sproule, G. J. Christianson, H. al Khabbaz, A. C. Brown, L. G. Presta, Y. G. Meng, D. C. Roopenian, Enhanced half-life of genetically engineered human IgG1 antibodies in a humanized FcRn mouse model: Potential application in humorally mediated autoimmune disease. *Int. Immunol.* **18**, 1759–1769 (2006).

32. G. Shankar, S. Arkin, L. Cocea, V. Devanarayan, S. Kirshner, A. Kromminga, V. Quarmby, S. Richards, C. K. Schneider, M. Subramanyam, S. Swanson, D. Verthelyi, S. Yim; American Association of Pharmaceutical Scientists, Assessment and reporting of the clinical immunogenicity of therapeutic proteins and peptides-harmonized terminology and tactical recommendations. *AAPS J.* **16**, 658–673 (2014).

33. K. M. Sand, B. Dalhus, G. J. Christianson, M. Bern, S. Foss, J. Cameron, D. Sleep, M. Bjørås, D. C. Roopenian, I. Sandlie, J. T. Andersen, Dissection of the neonatal Fc receptor (FcRn)-albumin interface using mutagenesis and anti-FcRn albumin-blocking antibodies. *J. Biol. Chem.* **289**, 17228–17239 (2014).

34. A. Grevys, J. Nilsen, K. M. K. Sand, M. B. Daba, I. Øynebråten, M. Bern, M. B. McAdam, S. Foss, T. Schlothauer, T. E. Michaelsen, G. J. Christianson, D. C. Roopenian, R. S. Blumberg, I. Sandlie, J. T. Andersen, A human endothelial cell-based recycling assay for screening of FcRn targeted molecules. *Nat. Commun.* **9**, 621 (2018).

35. H. H. Euler, P. Kern, H. Loffler, M. Dietrich, Precipitable immune complexes in healthy homosexual men, acquired immune deficiency syndrome and the related lymphadenopathy syndrome. *Clin. Exp. Immunol.* **59**, 267–275 (1985).

36. M. H. Tao, S. L. Morrison, Studies of aglycosylated chimeric mouse-human IgG. Role of carbohydrate in the structure and effector functions mediated by the human IgG constant region. *J. Immunol.* **143**, 2595–2601 (1989).

37. J. F. Liu, W. X. Wang, J. Xue, C. B. Zhao, H. Z. You, J. H. Lu, Y. Gu, Comparing the autoantibody levels and clinical efficacy of double filtration plasmapheresis, immunoadsorption, and intravenous immunoglobulin for the treatment of late-onset myasthenia gravis. *Ther. Apher. Dial.* **14**, 153–160 (2009).

38. W. Kohler, C. Bucka, R. Klingel, A randomized and controlled study comparing immunoadsorption and plasma exchange in myasthenic crisis. *J. Clin. Apher.* **26**, 347–355 (2011).

39. A. Kasuya, A. Moriki, K. Tatsuno, S. Hirakawa, Y. Tokura, Clearance efficacy of autoantibodies in double filtration plasmapheresis for pemphigus foliaceus. *Acta Derm. Venereol.* **93**, 181–182 (2013).

40. V. P. Werth, D. Culton, L. Blumberg, J. Humphries, R. Blumberg, R. Hall, 538 FcRn blockade with SYNT001 for the treatment of pemphigus. *J. Investig. Dermatol.* **138**, S92 (2018).

41. T. S. Ipe, M. B. Marques, Vascular access for therapeutic plasma exchange. *Transfusion* **58**, 580–589 (2018).

42. F. Olaru, W. Luo, H. Suleiman, P. L. St. John, L. Ge, A. R. Mezo, A. S. Shaw, D. R. Abrahamson, J. H. Miner, D. B. Borza, Neonatal Fc receptor promotes immune complex-mediated glomerular disease. *J. Am. Soc. Nephrol.* **25**, 918–925 (2014).

43. M. M. Barros, M. A. Blajchman, J. O. Bordin, Warm autoimmune hemolytic anemia: Recent progress in understanding the immunobiology and the treatment. *Transfus. Med. Rev.* **24**, 195–210 (2010).

44. K. Kobayashi, S. W. Qiao, M. Yoshida, K. Baker, W. I. Lencer, R. S. Blumberg, An FcRn-dependent role for anti-flagellin immunoglobulin G in pathogenesis of colitis in mice. *Gastroenterology* **137**, 1746–1756.e1 (2009).

45. R. J. Ober, C. Martinez, X. Lai, J. Zhou, E. S. Ward, Exocytosis of IgG as mediated by the receptor, FcRn: An analysis at the single-molecule level. *Proc. Natl. Acad. Sci. U.S.A.* **101**, 11076–11081 (2004).

46. H. P. Montoyo, C. Vaccaro, M. Hafner, R. J. Ober, W. Mueller, E. S. Ward, Conditional deletion of the MHC class I-related receptor FcRn reveals the sites of IgG homeostasis in mice. *Proc. Natl. Acad. Sci. U.S.A.* **106**, 2788–2793 (2009).

47. J. A. Kenniston, B. M. Taylor, G. P. Conley, J. Cosic, K. J. Kopacz, A. P. Lindberg, S. R. Comeau, K. Atkins, J. Bullen, C. TenHoor, B. A. Adelman, D. J. Sexton, T. E. Edwards, A. E. Nixon, Structural basis for pH-insensitive inhibition of immunoglobulin G recycling by an anti-neonatal Fc receptor antibody. *J. Biol. Chem.* **292**, 17449–17460 (2017).

48. S. Angal, D. J. King, M. W. Bodmer, A. Turner, A. D. G. Lawson, G. Roberts, B. Pedley, J. R. Adair, A single amino acid substitution abolishes the heterogeneity of chimeric mouse/human (IgG4) antibody. *Mol. Immunol.* **30**, 105–108 (1993).

49. J. Running Deer, D. S. Allison, High-level expression of proteins in mammalian cells using transcription regulatory sequences from the Chinese hamster EF-1α gene. *Biotechnol. Prog.* **20**, 880–889 (2004).

50. Z. Assur, W. A. Hendrickson, F. Mancia, Tools for coproducing multiple proteins in mammalian cells. *Methods Mol. Biol.* **801**, 173–187 (2012).

51. M. C. Franklin, M. J. Rudolph, C. Ginter, M. S. Cassidy, J. Cheung, Structures of paraoxon-inhibited human acetylcholinesterase reveal perturbations of the acyl loop and the dimer interface. *Proteins* **84**, 1246–1256 (2016).

52. J. Cheung, M. J. Rudolph, F. Burshteyn, M. S. Cassidy, E. N. Gary, J. Love, M. C. Franklin, J. J. Height, Structures of human acetylcholinesterase in complex with pharmacologically important ligands. *J. Med. Chem.* **55**, 10282–10286 (2012).

53. Z. Otwinowski, W. Minor, Processing of x-ray diffraction data collected in oscillation mode. *Methods Enzymol.* **276**, 307–326 (1997).

54. M. D. Winn, C. C. Ballard, K. D. Cowtan, E. J. Dodson, P. Emsley, P. R. Evans, R. M. Keegan, E. B. Krissinel, A. G. W. Leslie, A. McCoy, S. J. McNicholas, G. N. Murshudov, N. S. Pannu, E. A. Potterton, H. R. Powell, R. J. Read, A. Vagin, K. S. Wilson, Overview of the CCP4 suite and current developments. *Acta Crystallogr., Sect. D: Biol. Crystallogr.* **67**, 235–242 (2011).

55. A. J. McCoy, R. W. Grosse-Kunstleve, P. D. Adams, M. D. Winn, L. C. Storoni, R. J. Read, Phaser crystallographic software. *J. Appl. Cryst.* **40**, 658–674 (2007).

56. P. Emsley, B. Lohkamp, W. G. Scott, K. Cowtan, Features and development of Coot. *Acta Crystallogr., Sect. D: Biol. Crystallogr.* **66**, 486–501 (2010).

57. P. D. Adams, P. V. Afonine, G. Bunkóczi, V. B. Chen, I. W. Davis, N. Echols, J. J. Headd, L. W. Hung, G. J. Kapral, R. W. Grosse-Kunstleve, A. J. McCoy, N. W. Moriarty, R. Oeffner, R. J. Read, D. C. Richardson, J. S. Richardson, T. C. Terwilliger, P. H. Zwart, PHENIX: A comprehensive Python-based system for macromolecular structure solution. *Acta Crystallogr., Sect. D: Biol. Crystallogr.* **66**, 213–221 (2010).

58. D. C. Roopenian, G. J. Christianson, T. J. Sproule, A. C. Brown, S. Akilesh, N. Jung, S. Petkova, L. Avanessian, E. Y. Choi, D. J. Shaffer, P. A. Eden, C. L. Anderson, The MHC class I-like IgG receptor controls perinatal IgG transport, IgG homeostasis, and fate of IgG-Fc-coupled drugs. *J. Immunol.* **170**, 3528–3533 (2003).

59. M. Yoshida, S. M. Claypool, J. S. Wagner, E. Mizoguchi, A. Mizoguchi, D. C. Roopenian, W. I. Lencer, R. S. Blumberg, Human neonatal Fc receptor mediates transport of IgG into luminal secretions for delivery of antigens to mucosal dendritic cells. *Immunity* **20**, 769–783 (2004).

60. G. J. Christianson, V. Z. Sun, S. Akilesh, E. Pesavento, G. Proetzel, D. C. Roopenian, Monoclonal antibodies directed against human FcRn and their applications. *MAbs* **4**, 208–216 (2014).

Citation: L. J. Blumberg, J. E. Humphries, S. D. Jones, L. B. Pearce, R. Holgate, A. Hearn, J. Cheung, A. Mahmood, B. Del Tito, J. S. Graydon, L. E. Stolz, A. Bitonti, S. Purohit, D. de Graaf, K. Kacena, J. T. Andersen, G. J. Christianson, D. C. Roopenian, J. J. Hubbard, A. K. Gandhi, K. Lasseter, M. Pyzik, R. S. Blumberg, Blocking FcRn in humans reduces circulating IgG levels and inhibits IgG immune complex–mediated immune responses. *Sci. Adv.* **5**, eaax9586 (2019).